X-ray spectroscopy of the brightest gamma-ray nova ASASSN-18fv = N Car 18 = V906 Car

Kirill Sokolovsky *Michigan State University, SAI Moscow State Univ., ASC Lebedev* in collaboration with
Elias Aydi, Laura Chomiuk, Adam Kawash *Michigan State Univ.,*
Koji Mukai *NASA/GSFC,* Raimundo Lopes *Universidade Federal de Sergipe,* Thomas Nelson *Univ. of Pittsburgh,*
Brian D. Metzger, Elad Steinberg *Columbia University*

Nova Car 2018 and η Car nebula
imaged by Joseph Brimacombe

Classical novae emit X-rays

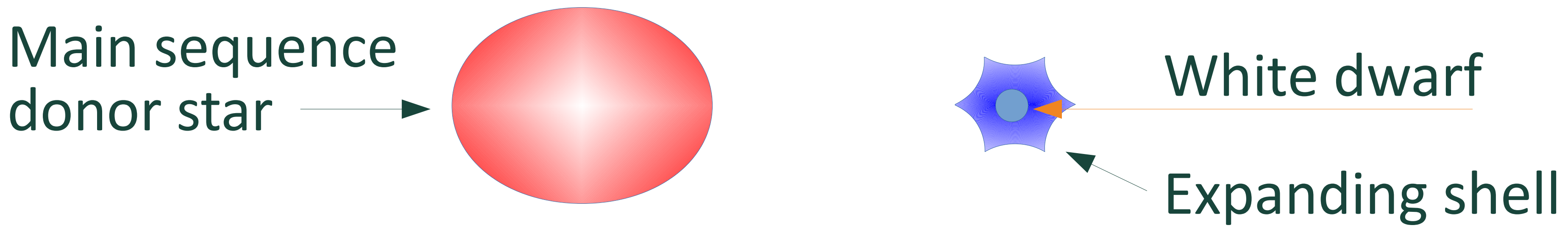

1) **X-ray fireball in first hours of explosion,** never observed
2) Shock waves heat plasma and accelerate particles weeks
months after explosion
3) Hydrogen-burning white dwarf - “Super-Soft Source”
4) When accretion restarts, the gas hitting WD surface gets
shocked and heated to X-ray temperatures

Classical novae emit X-rays

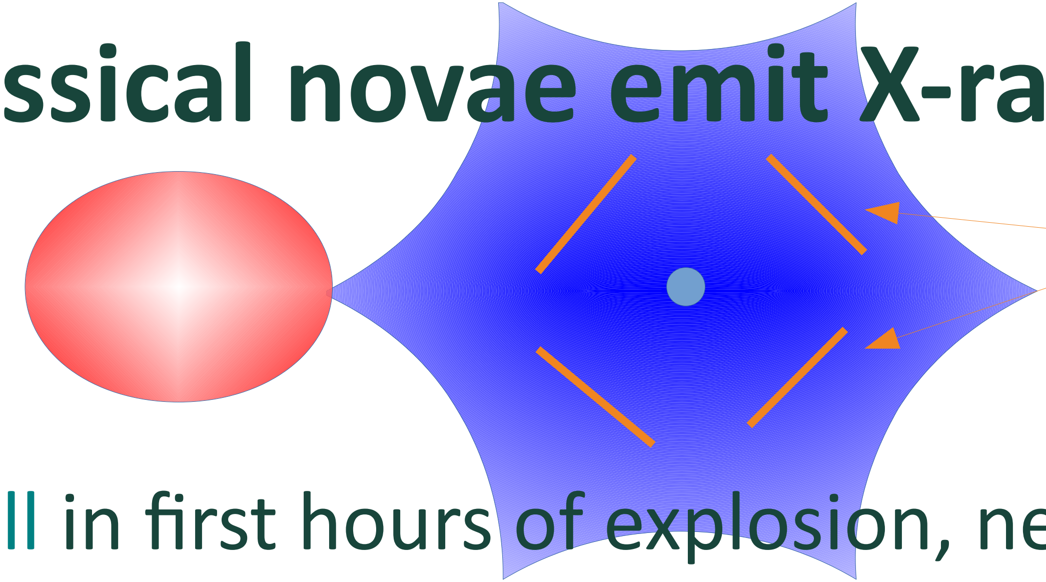

1) X-ray fireball in first hours of explosion, never observed

2) Shock waves heat plasma and accelerate particles weeks-months after explosion

3) Hydrogen-burning white dwarf - "Super-Soft Source"

4) When accretion restarts, the gas hitting WD surface gets shocked and heated to X-ray temperatures

Classical novae emit X-rays

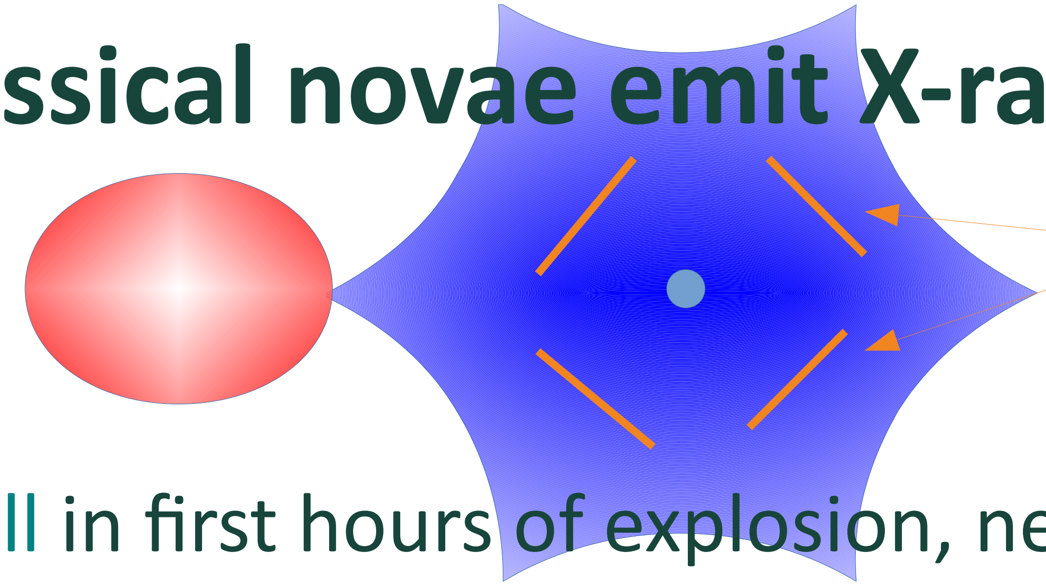

1) X-ray fireball in first hours of explosion, never observed

2) Shock waves heat plasma and accelerate particles weeks-months after explosion

Poster by A. Muethel

3) Hydrogen-burning white dwarf - “Super-Soft Source”

4) When accretion restarts, the gas hitting WD surface gets shocked and heated to X-ray temperatures

Classical novae emit X-rays

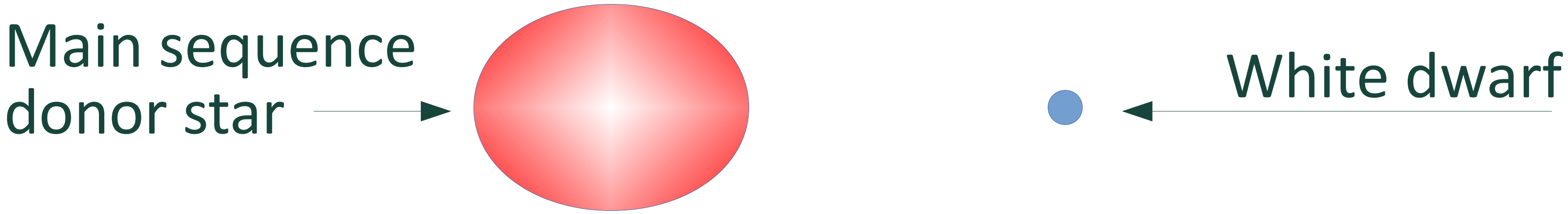

1) X-ray fireball in first hours of explosion, never observed
2) Shock waves heat plasma and accelerate particles weeks-months after explosion
3) **Hydrogen-burning white dwarf - “Super-Soft Source”**
4) When accretion restarts, the gas hitting WD surface gets shocked and heated to X-ray temperatures

Classical novae emit X-rays

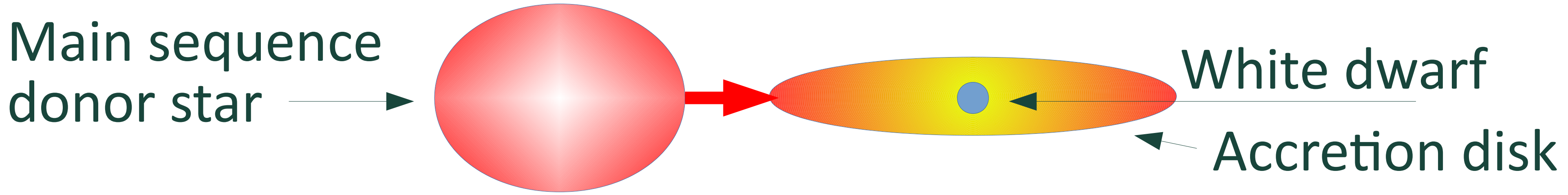

1) X-ray fireball in first hours of explosion, never observed
2) Shock waves heat plasma and accelerate particles weeks-months after explosion
3) Hydrogen-burning white dwarf - "Super-Soft Source"
4) **When accretion restarts, the gas hitting WD surface gets shocked and heated to X-ray temperatures**

ASASSN-18fv = N Car 2018 = V906 Car

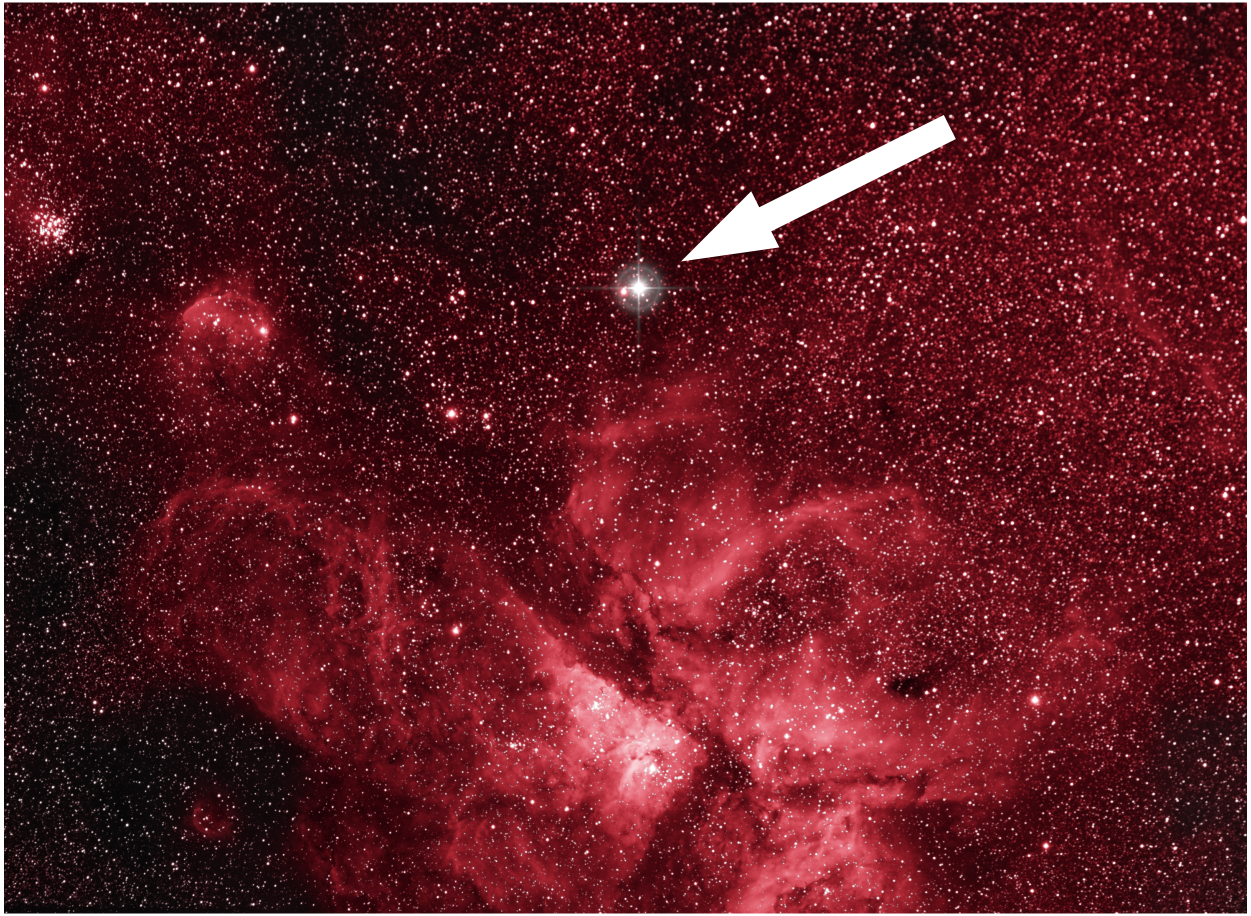

ASASSN-18fv and η Car nebula imaged by Joseph Brimacombe

Discovered 2018-03-20.32 UT
by the **ASAS-SN survey**

Opical/γ-ray lightcurve of V906 Car

BRITE
optical

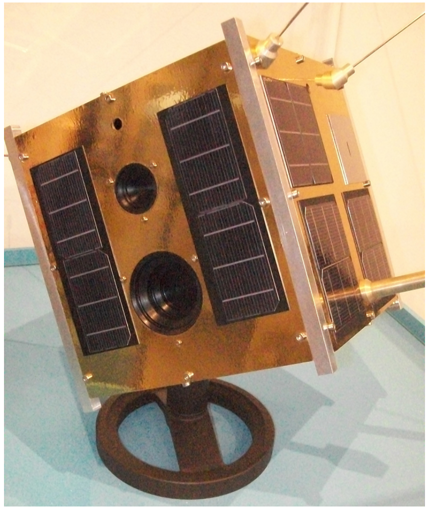

Fermi-LAT
100 MeV - 300 GeV

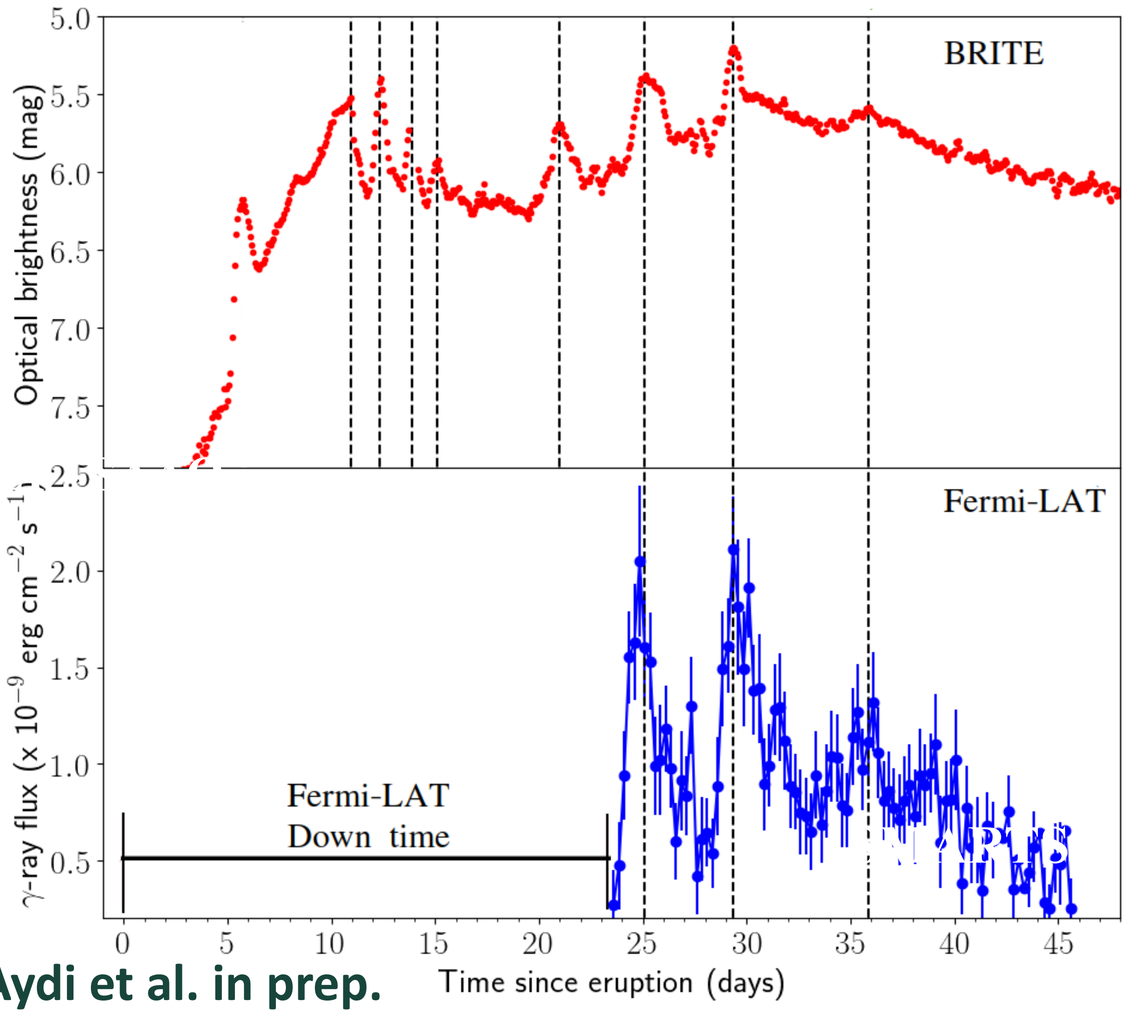

Aydi et al. in prep.

Opical/γ-ray lightcurve of V906 Car

BRITE
optical

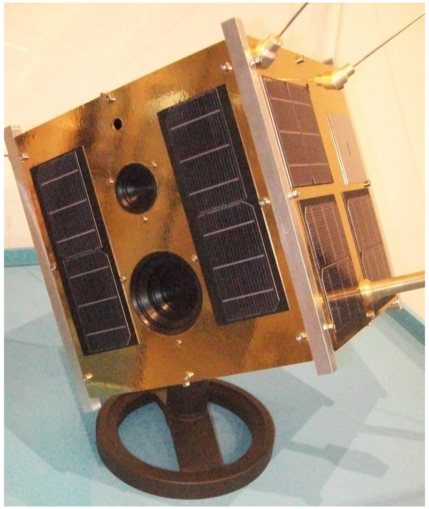

Fermi-LAT
100 MeV - 300 GeV

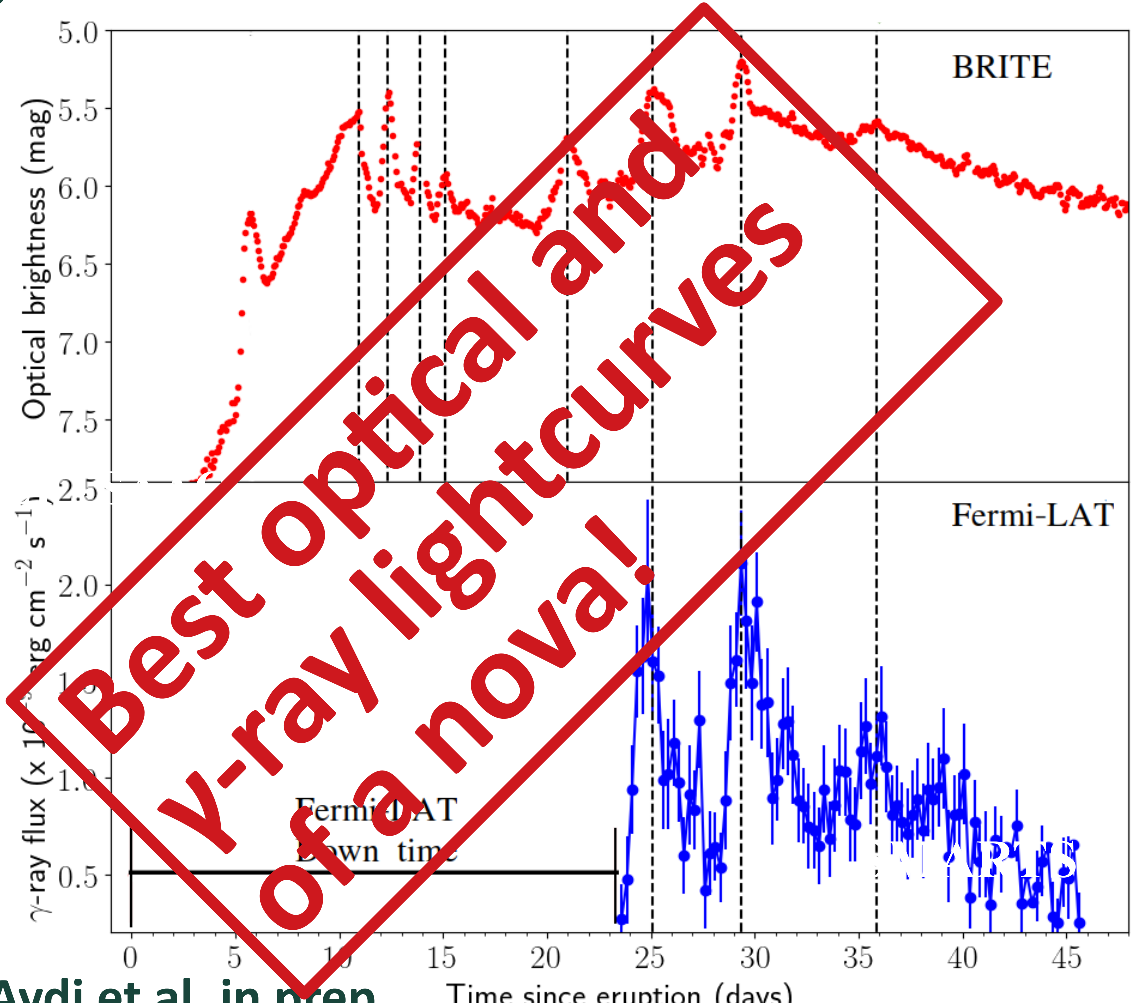

Aydi et al. in prep.

X-ray observations of V906 Car

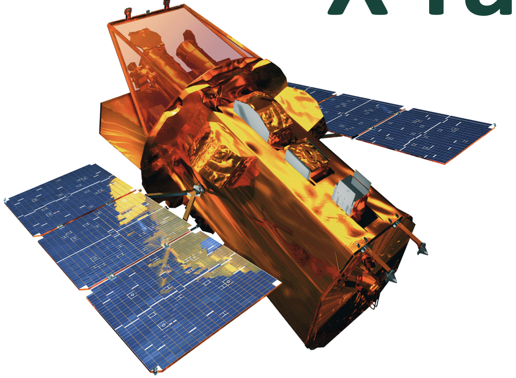

Swift (0.3–10 keV): fast repointing -> can do long-term monitoring

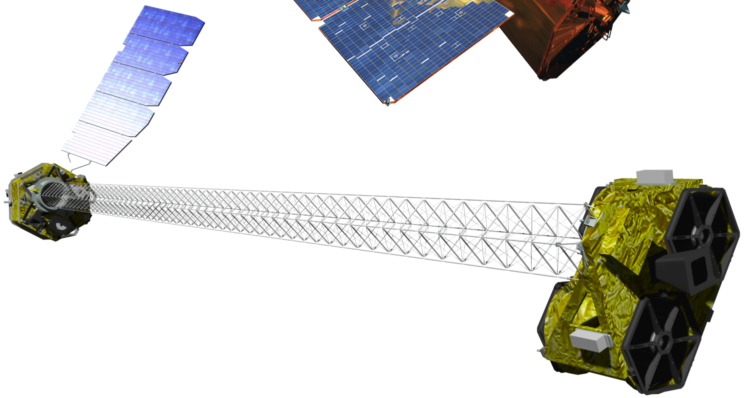

NuSTAR (3–78 keV): high sensitivity to hard X-rays

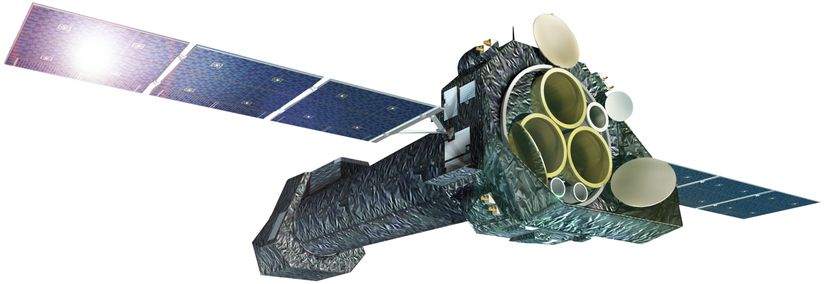

XMM-Newton: high-resolution spectroscopy (0.33–2.1 keV) with X-ray gratings + high sensitivity at 0.3–10 keV

Multiavelengths emission from V906 Car

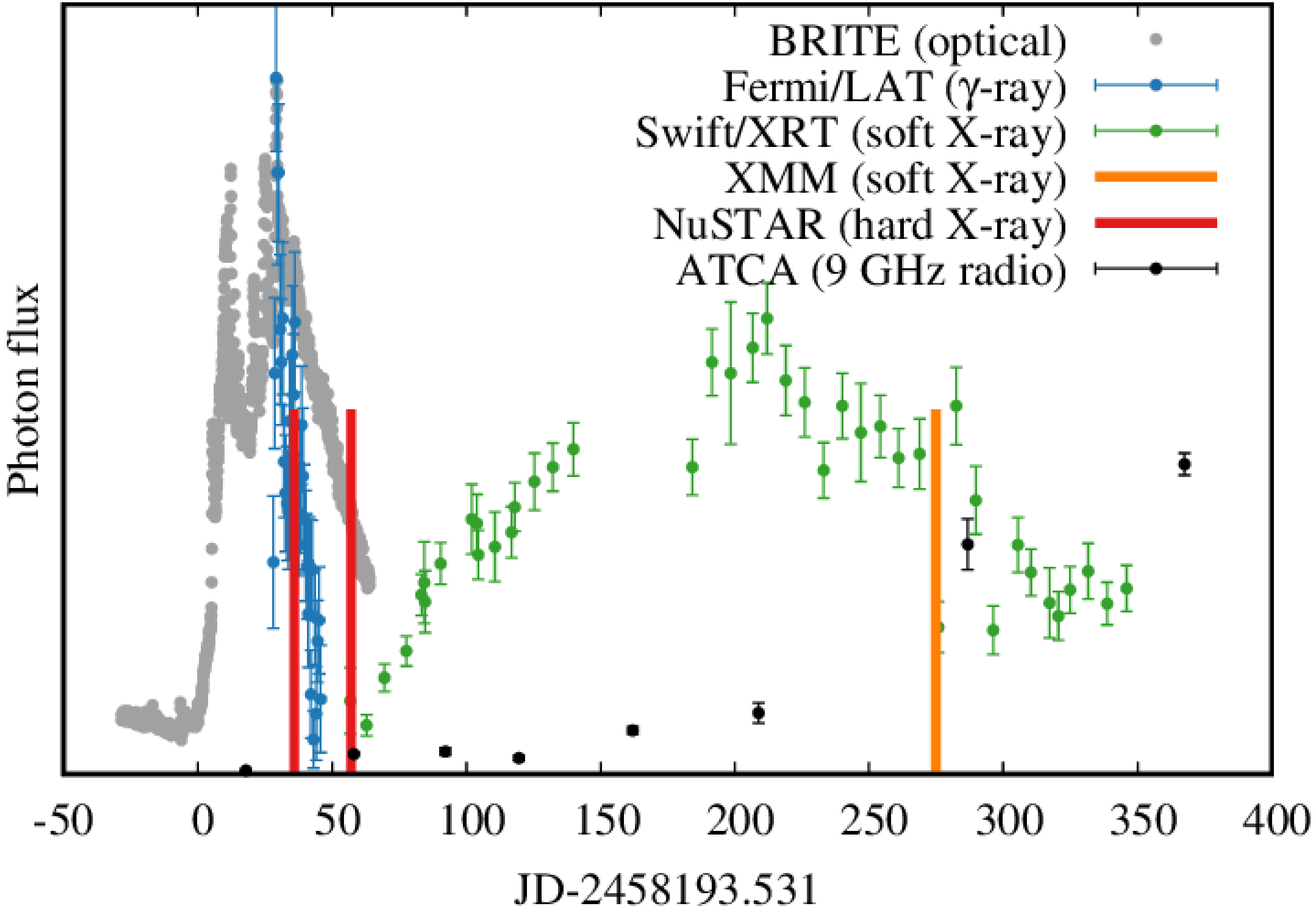

Swift lightcurve

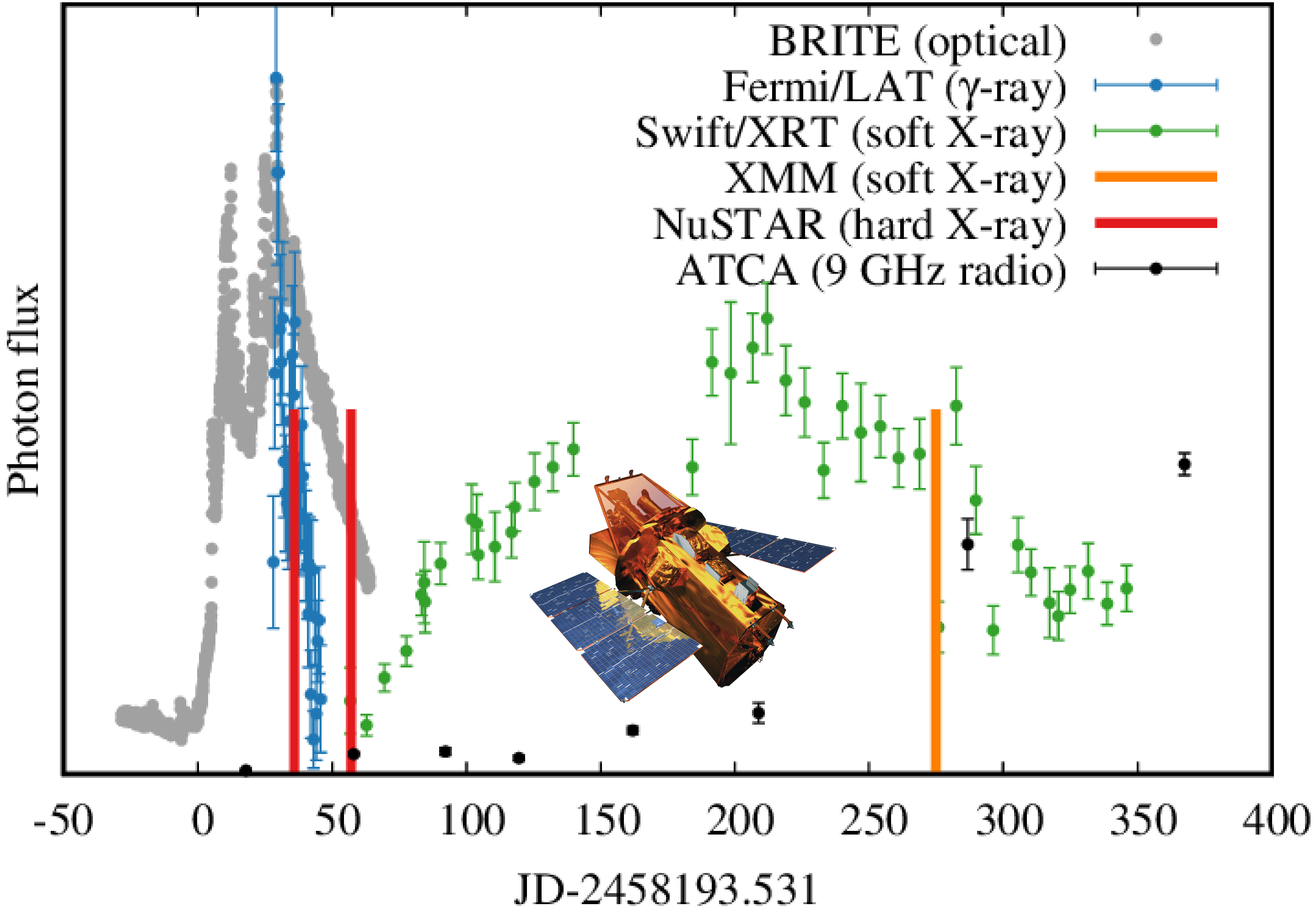

Swift/XRT lightcurve of V906 Car

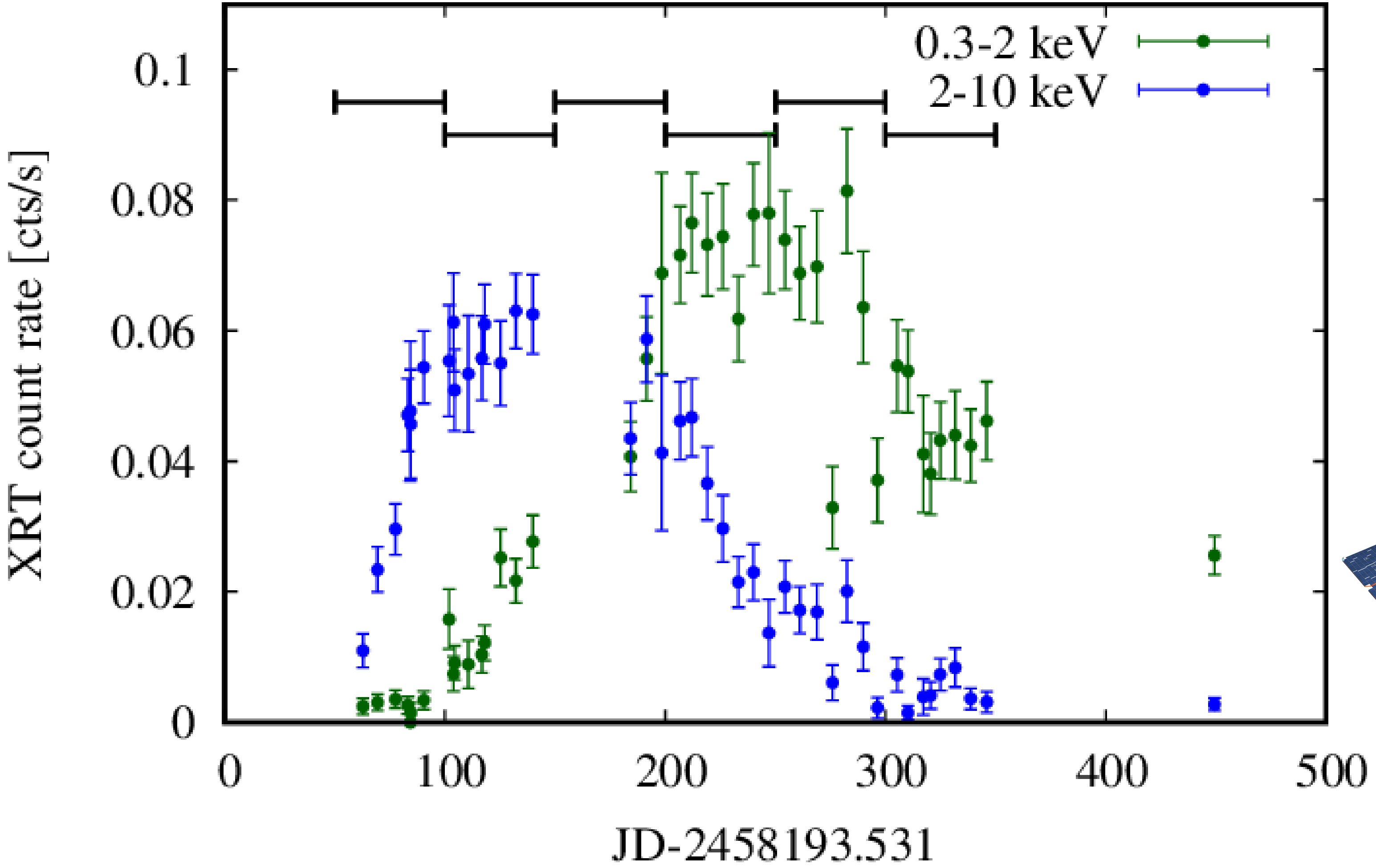

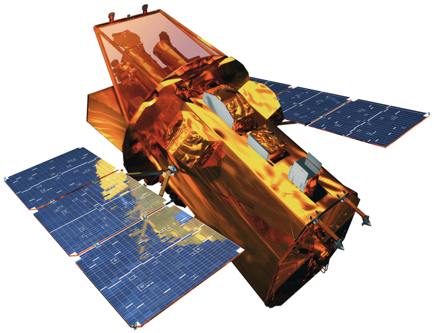

Swift/XRT lightcurve of V906 Car

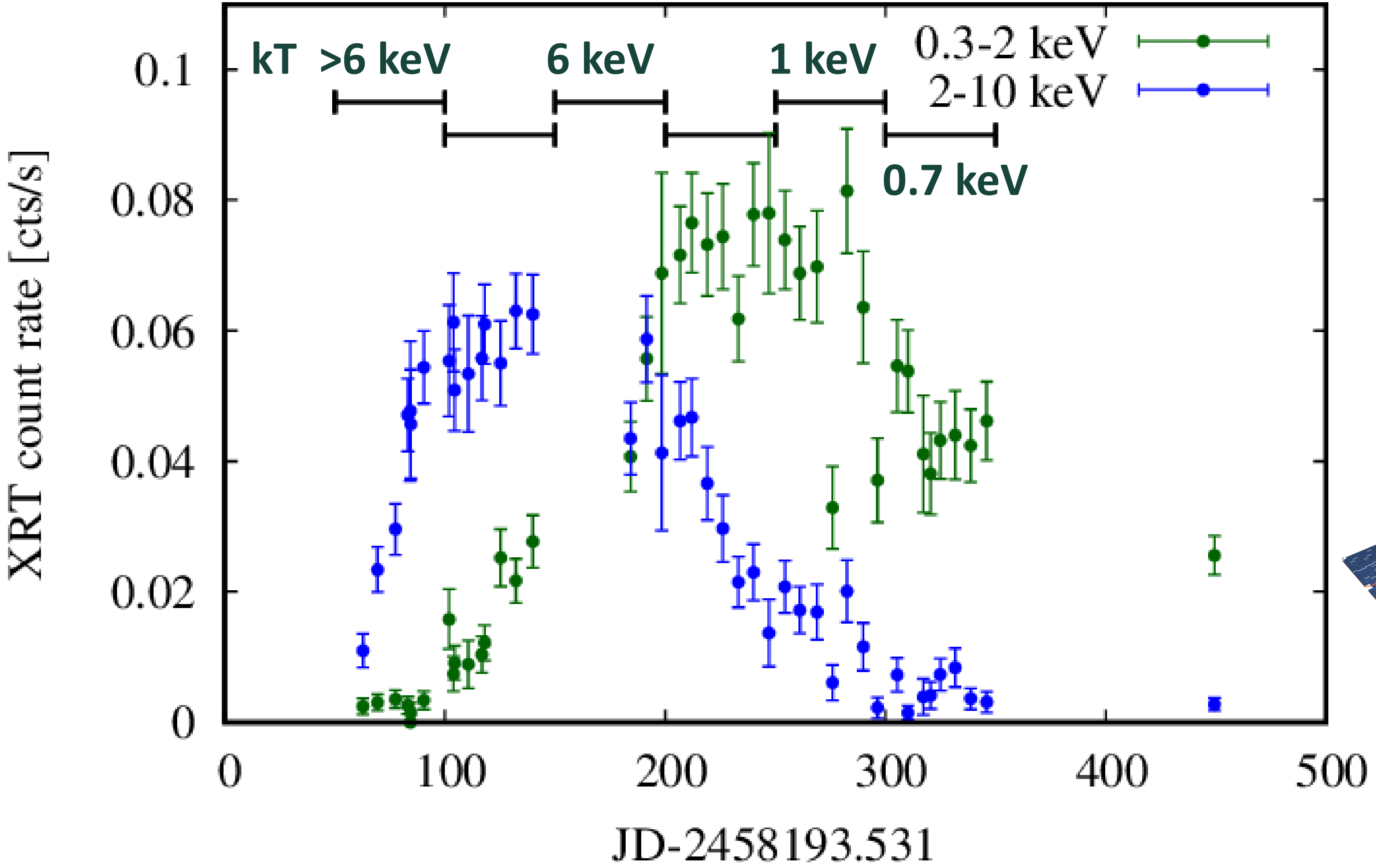

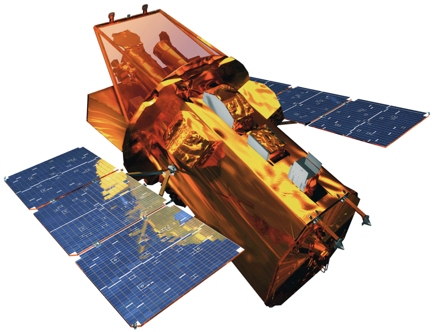

Swift/XRT lightcurve of V906 Car

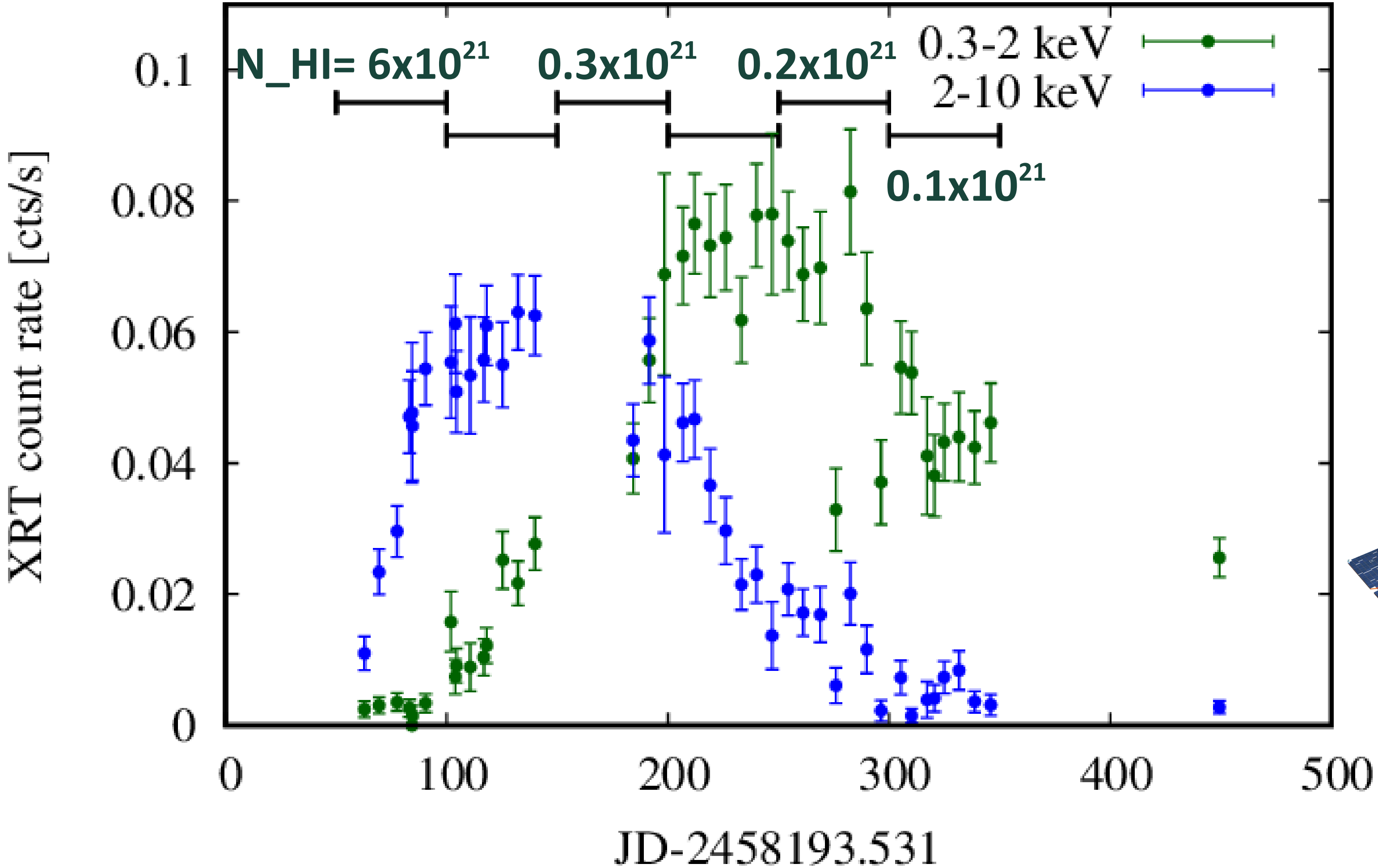

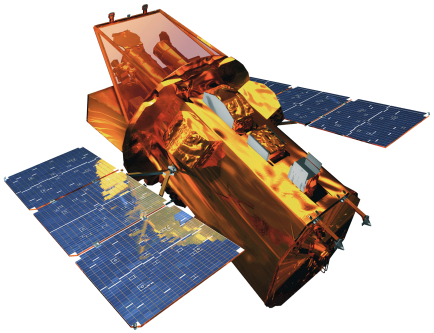

Late-time XMM obs. to get abundances

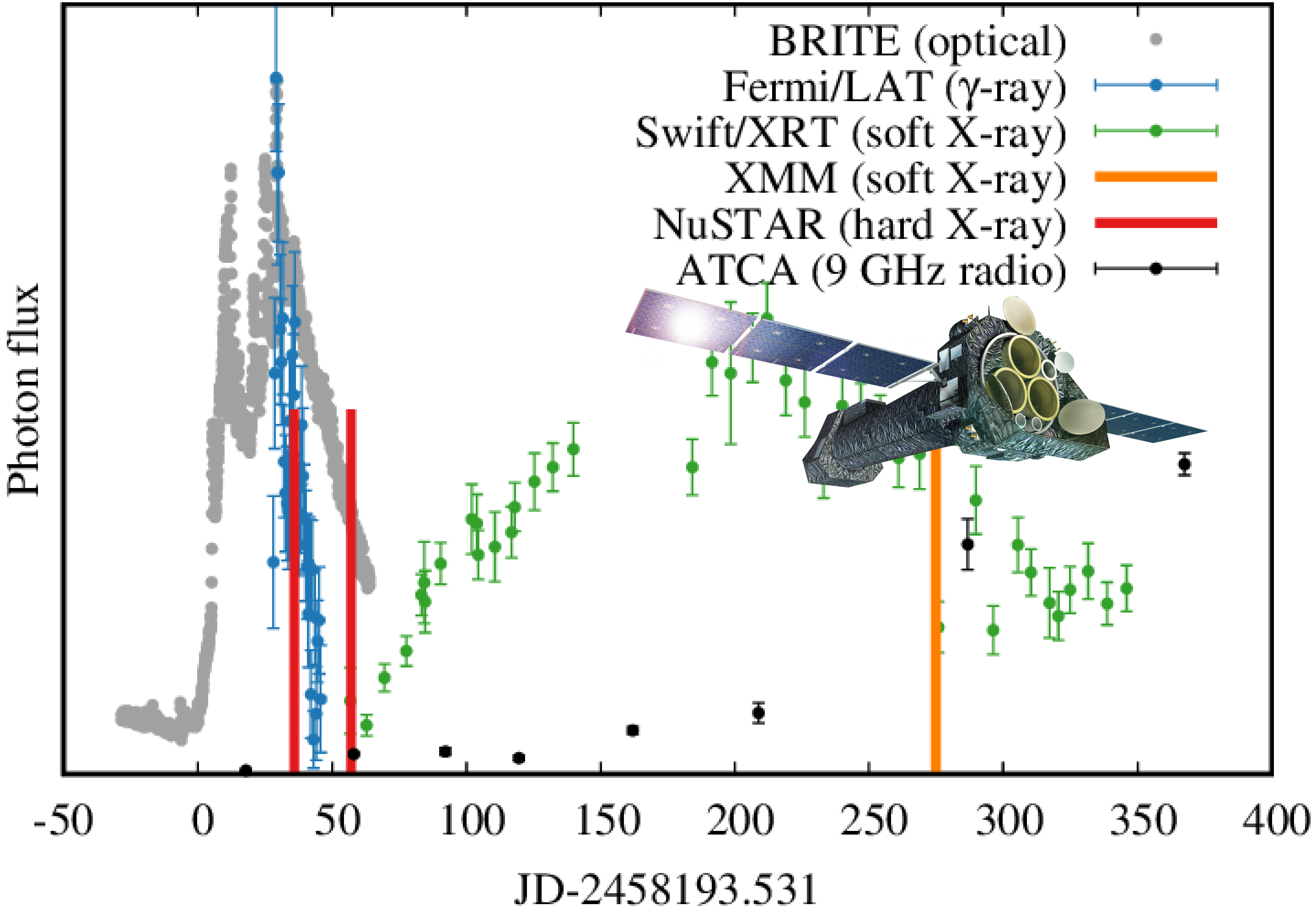

XMM/EPIC+RGS spectrum of V906 Car

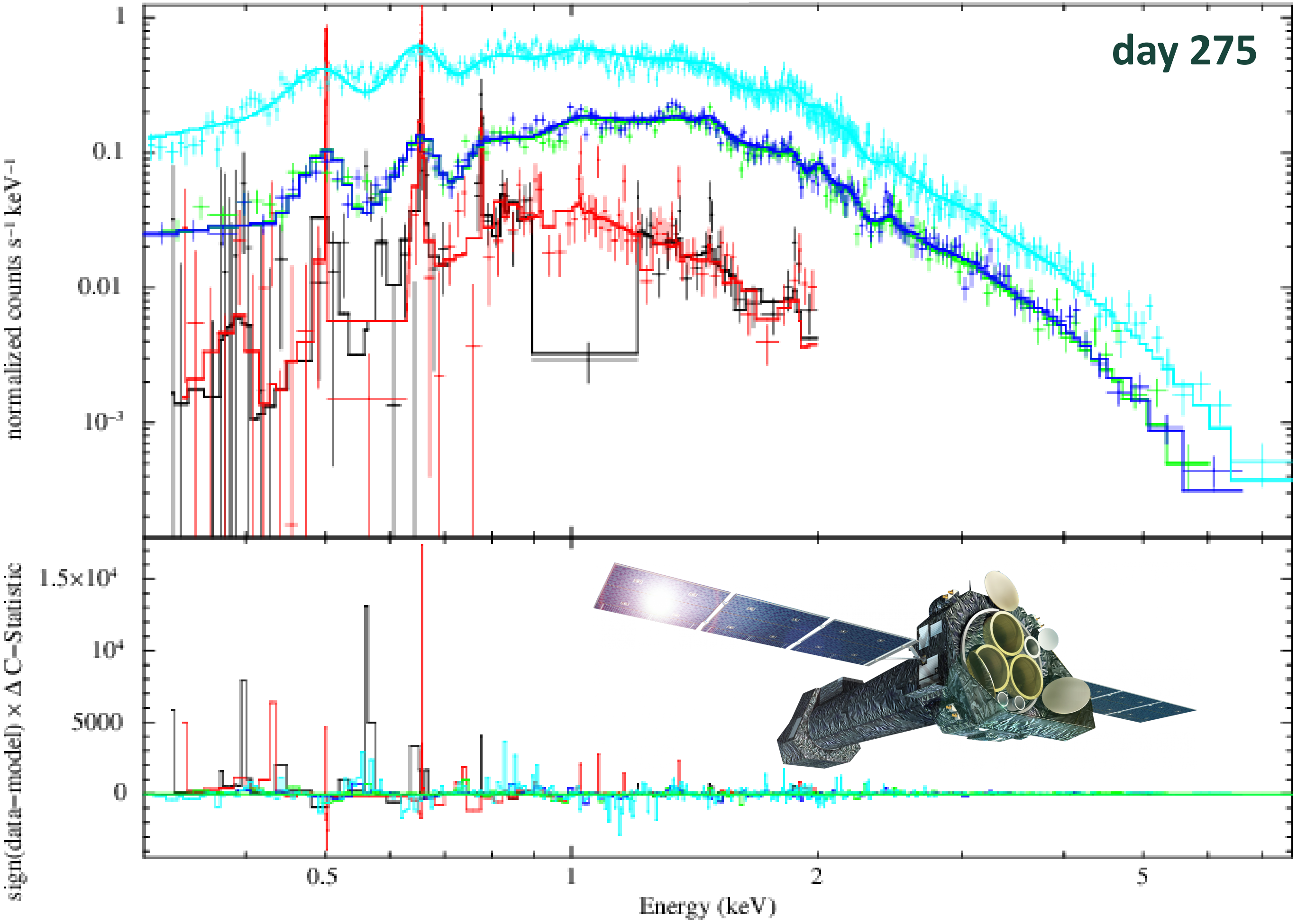


```
constant*phabs*vphabs*bvapec
```

	EPIC+RGS
PHABS	
N_H ($\times 10^{21}$ cm^{-2})	$2.4^{+0.4}_{-0.3}$
VPHABS	
N_H ($\times 10^{21}$ cm^{-2})	$0.12^{+0.03}_{-0.03}$
BVAPEC	
kT (keV)	$1.07^{+0.04}_{-0.01}$
redshift	$-2.9\times 10^{-3*}$
velocity (km s^{-1})	$378^{(*)}$
$N/N_\odot$	345^{+93}_{-70}
$O/O_\odot$	29^{+7}_{-5}
$Ne/Ne_\odot$	$2.2^{+0.6}_{-0.5}$
$Mg/Mg_\odot$	$0.6^{+0.2}_{-0.1}$
$Si/Si_\odot$	$1.1^{+0.2}_{-0.2}$
$Fe/Fe_\odot$	<0.1
χ^2_ν	1.15
d.o.f.	1837

XMM/EPIC+RGS spectrum of V906 Car

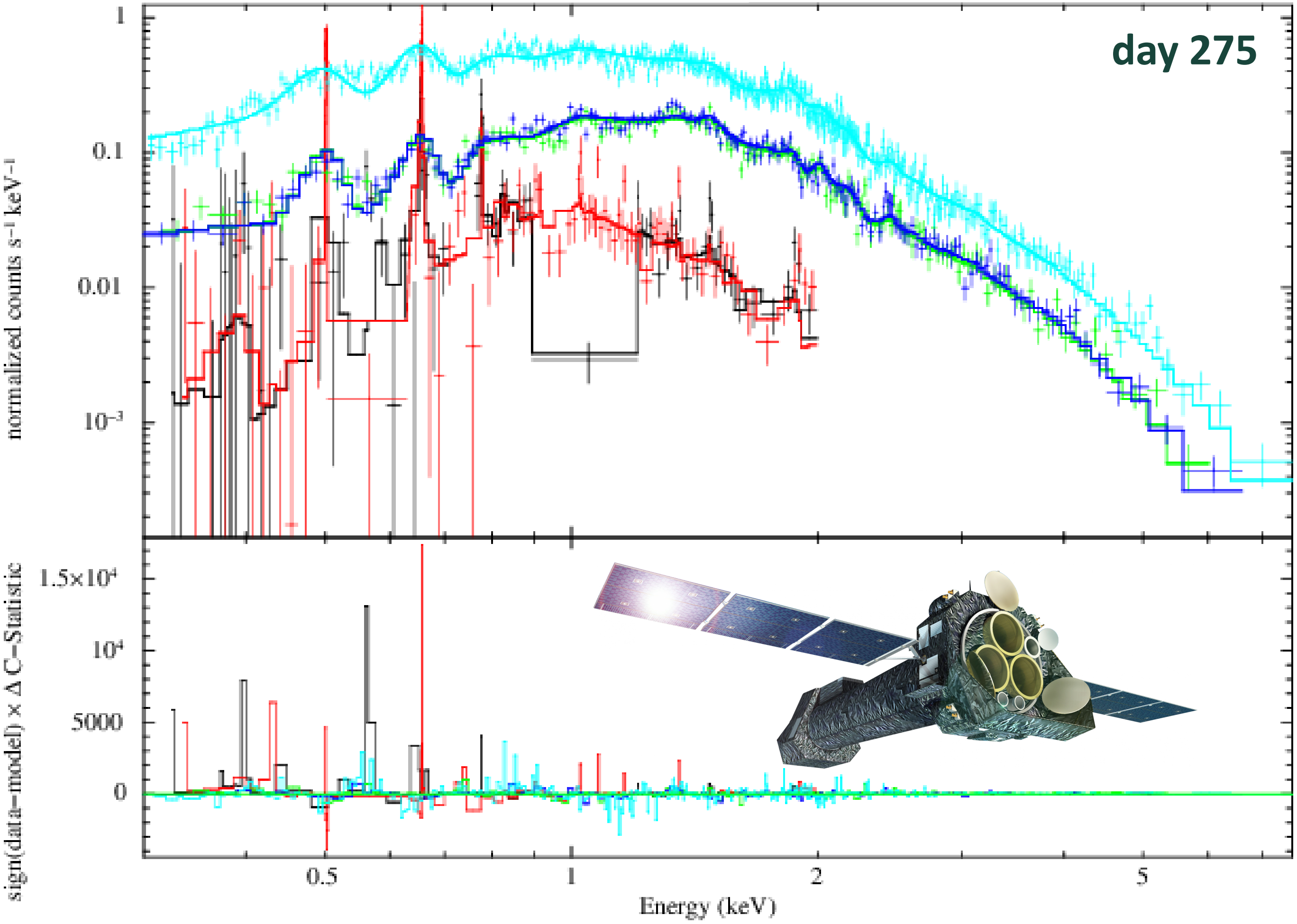

constant*phabs*vphabs*bvapec

	EPIC+RGS
PHABS	
N_H ($\times 10^{21}$ cm^{-2})	$2.4^{+0.4}_{-0.3}$
VPHABS	
N_H ($\times 10^{21}$ cm^{-2})	$0.12^{+0.03}_{-0.03}$
BVAPEC	
kT (keV)	$1.07^{+0.04}_{-0.01}$
redshift	$-2.9\times10^{-3*}$
velocity (km s^{-1})	$378^{(*)}$
$N/N_\odot$	345^{+93}_{-70}
$O/O_\odot$	29^{+7}_{-5}
$Ne/Ne_\odot$	$2.2^{+0.6}_{-0.5}$
$Mg/Mg_\odot$	$0.6^{+0.2}_{-0.1}$
$Si/Si_\odot$	$1.1^{+0.2}_{-0.2}$
$Fe/Fe_\odot$	<0.1
χ^2_ν	1.15
d.o.f.	1837

XMM/EPIC+RGS spectrum of V906 Car

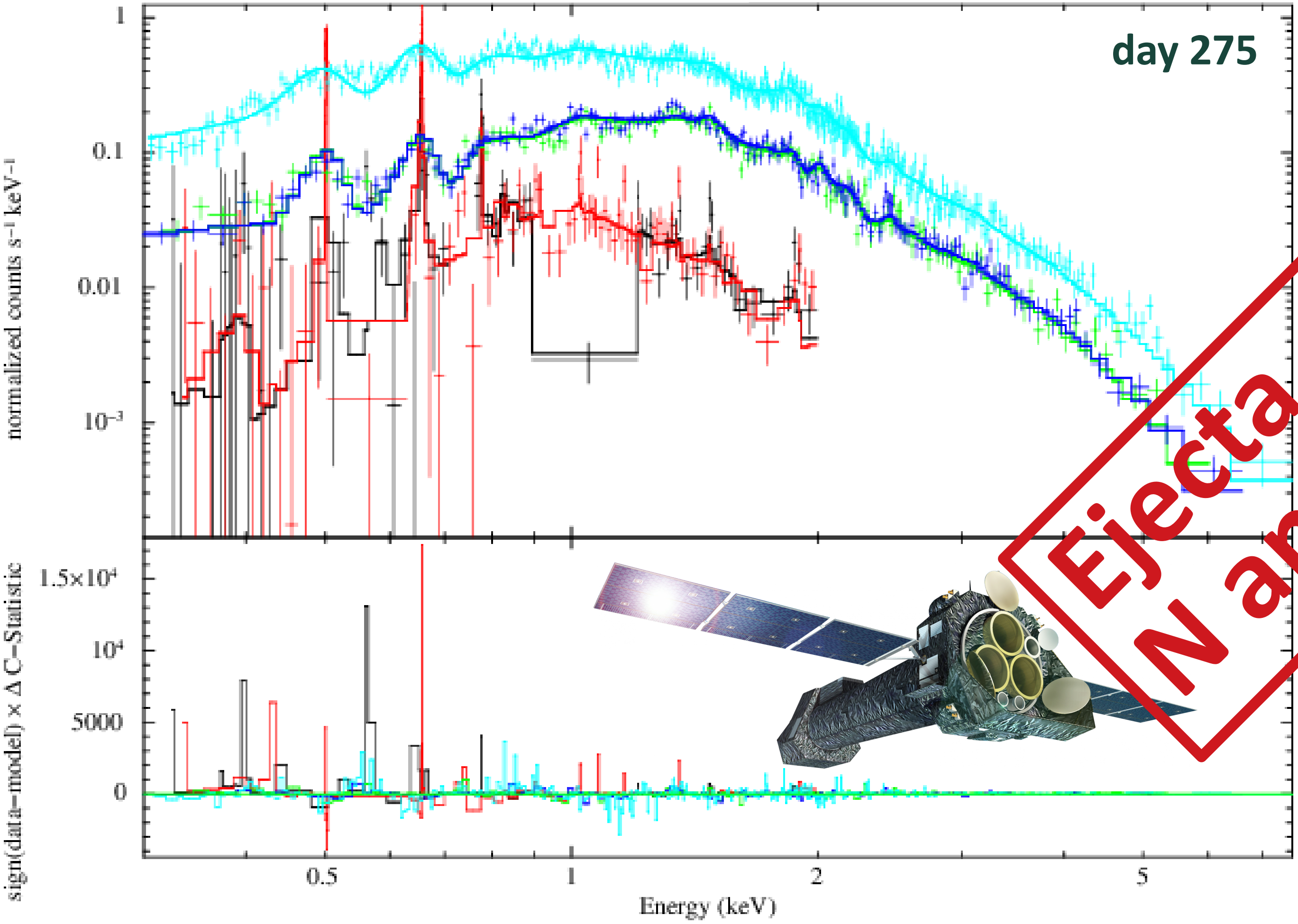

`constant*phabs*vphabs*bvapec`

	EPIC+RGS
PHABS	
N_H ($\times 10^{21}$ cm^{-2})	$2.4^{+0.4}_{-0.3}$
VPHABS	
N_H ($\times 10^{21}$ cm^{-2})	$0.12^{+0.03}_{-0.03}$
BVAPEC	
kT (keV)	$1.07^{+0.04}_{-0.01}$
redshift	$-2.9\times 10^{-3}*$
velocity (km s^{-1})	$378^{(*)}$
N/N$_\odot$	345^{+93}_{-70}
O/O$_\odot$	29^{+7}_{-5}
Ne/Ne$_\odot$	$2.2^{+0.6}_{-0.5}$
Mg/Mg$_\odot$	$0.6^{+0.2}_{-0.1}$
Si/Si$_\odot$	$1.1^{+0.2}_{-0.2}$
Fe/Fe$_\odot$	<0.1
χ^2_ν	1.15
d.o.f.	1837

Ejecta enriched in N and O, low Fe

Ejecta includes a lot of WD material

CNO cycle is a catalytic cycle, fusion in nova **does not enrich ejecta in CNO** elements, just alters relative abundances

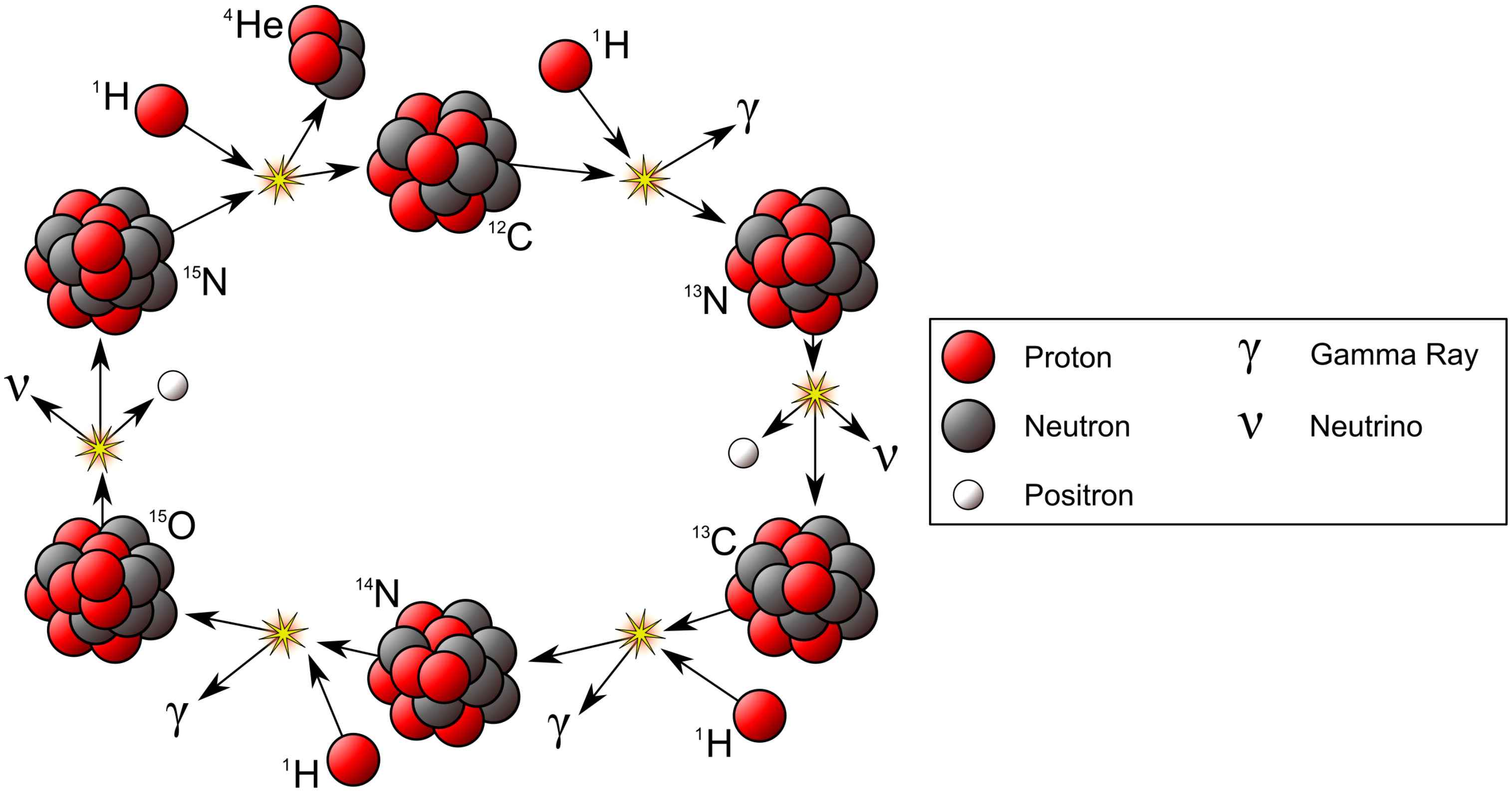

Ejecta includes a lot of WD material

so we can infer the WD composition! The absence of strong Mg and Ne emission suggests it's a **CO WD**, rather than ONe

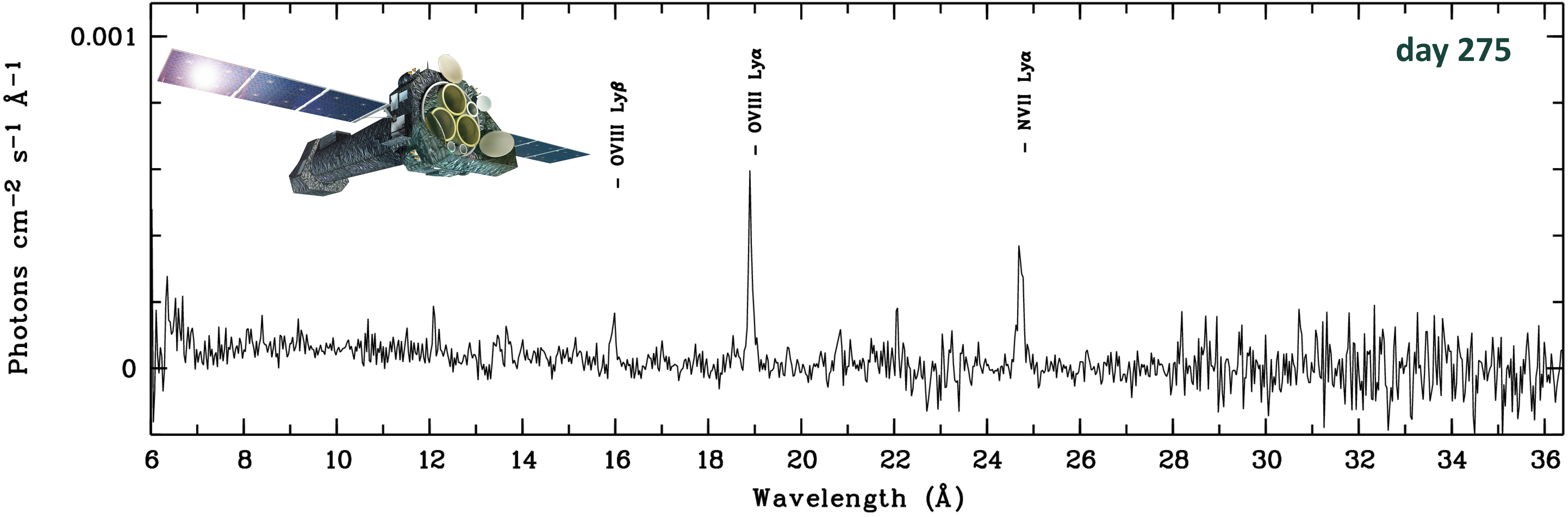

Two NuSTAR epochs

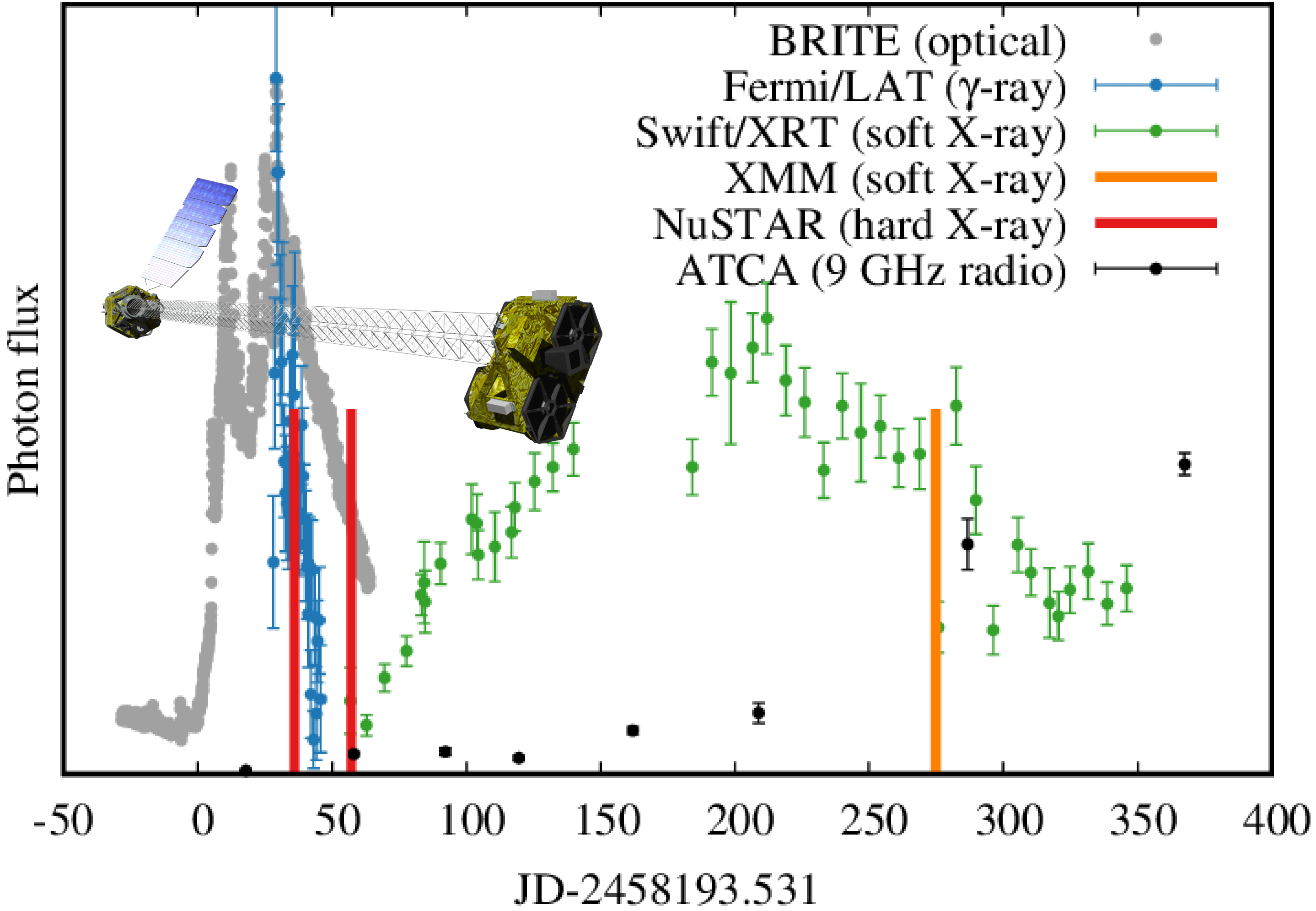

NuSTAR spectra of V906 Car

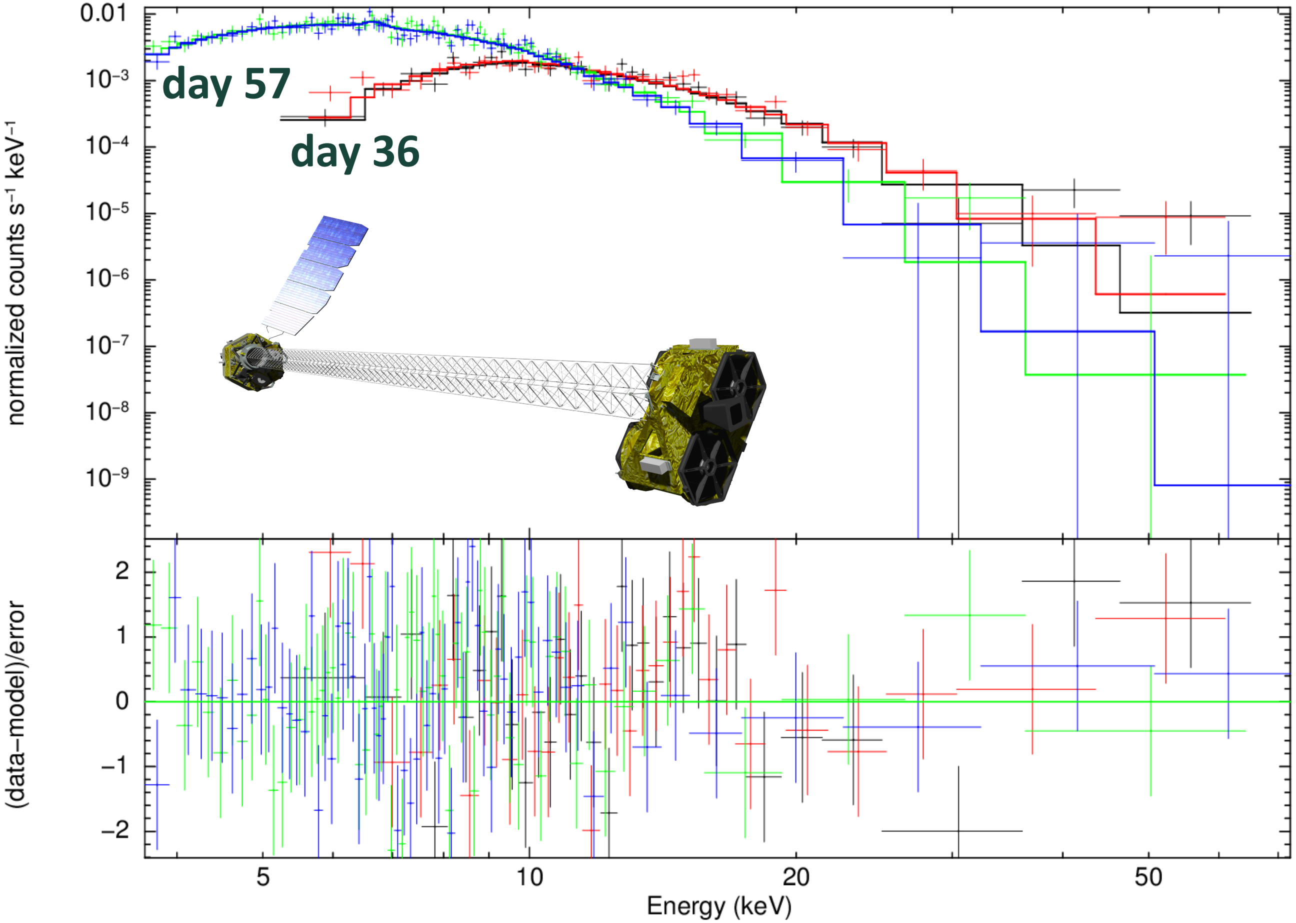

day 36:
kT = 8.6 +-0.9 keV
nHI = 19 +-1 x10^22 cm^-2
F = 2.7 x10^-12 ergs/s/cm^2

day 57:
kT = 4.3 +-0.2 keV
nHI = 2.6 +-0.2 x10^22 cm^-2
F = 3.5 x10^-12 ergs/s/cm^2

Overabundance by number w.r.t. solar:
C=0
O=29
N=345

no non-thermal emission

NuSTAR spectra of V906 Car

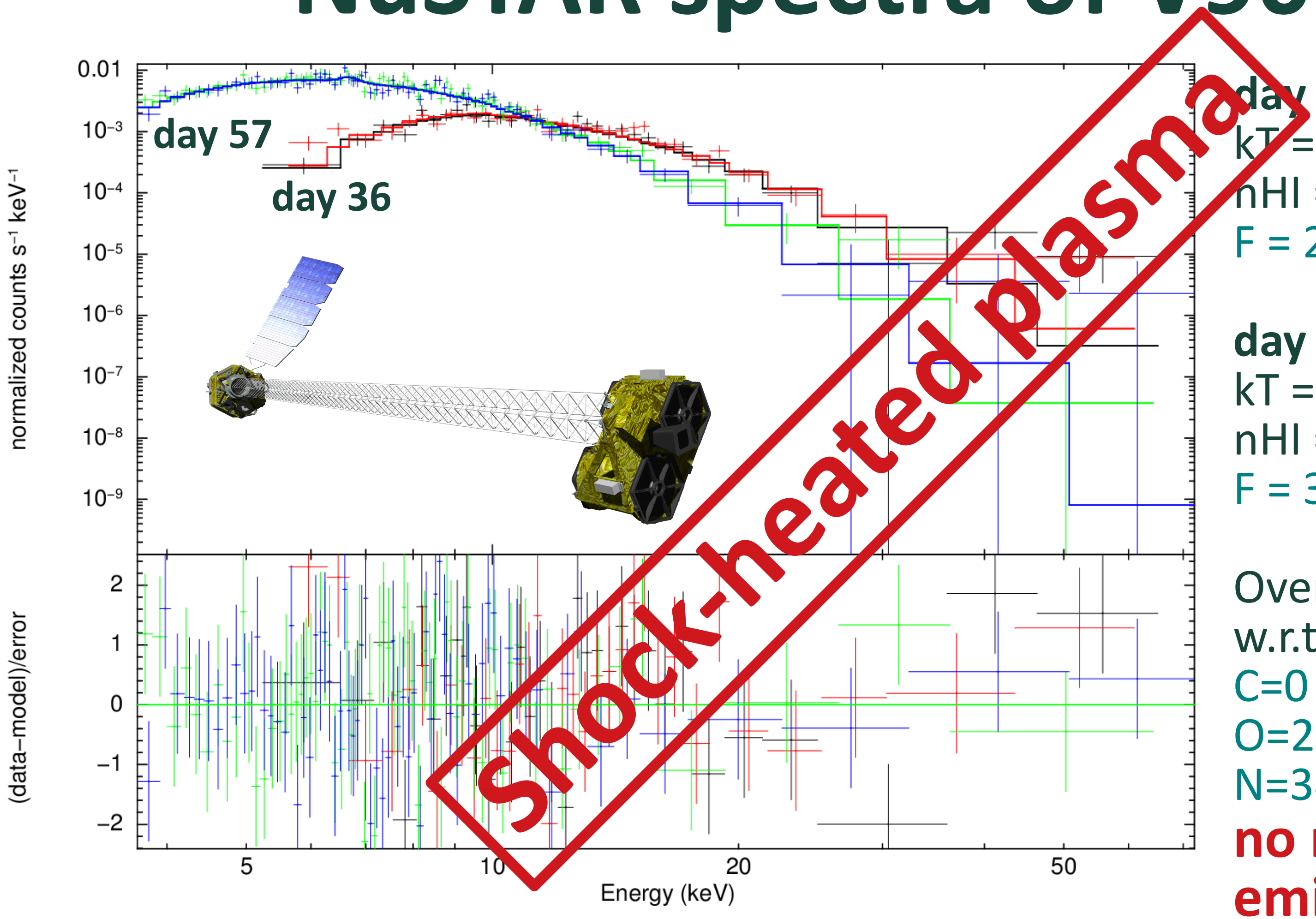

day 36:
kT = 8.6 +-0.9 keV
nHI = 19 +-1 x10^22 cm^-2
F = 2.7 x10^-12 ergs/s/cm^2

day 57:
kT = 4.3 +-0.2 keV
nHI = 2.6 +-0.2 x10^22 cm^-2
F = 3.5 x10^-12 ergs/s/cm^2

Overabundance by number w.r.t. solar:
C=0
O=29
N=345

no non-thermal emission

NuSTAR observations of novae

Five novae observed so far:

- **V745 Sco** (WD+RG) - detected (Orio et al. 2015)
- **V339 Del** - not detected (Mukai et al. in prep.)
- **V5668 Sgr** - not detected (Mukai et al. in prep.)
- **V5855 Sgr** - detected while still γ-ray bright (Nelson et al. 2019)
- **V906 Car** - detected while still γ-ray bright

Spectra consistent with thermal emission in all cases

Ejecta mass: Hubble flow model

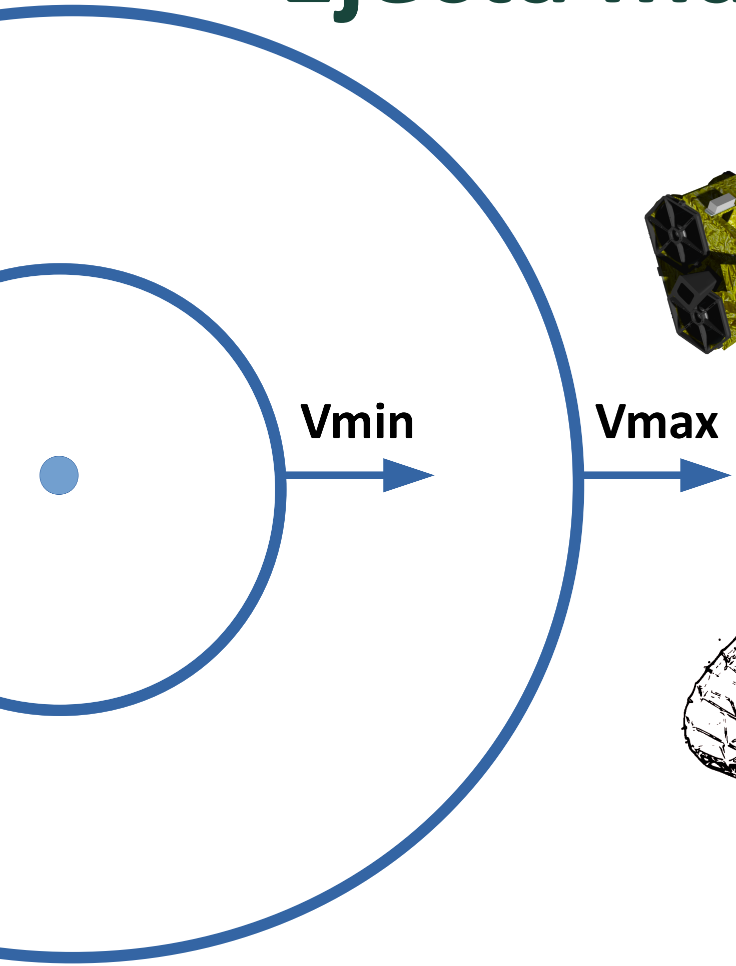

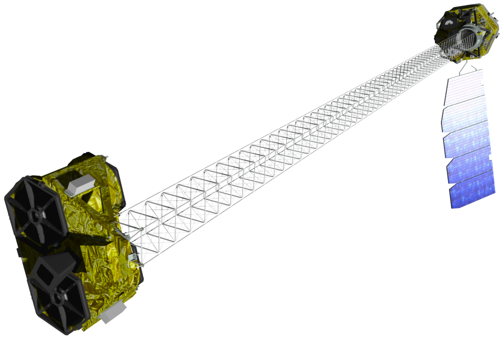

The inner/outer shell velocity ratios from the literature

Nova	$v_{\rm min}/v_{\rm max}$	Reference
V1324 Sco	$0.447^{+0.10}_{-0.079}$	Finzell et al. (2018)
V959 Mon	0.083	Chomiuk et al. (2014a)
V5589 Sgr	0.84	Weston et al. (2016b)
V1723 Aql	0.17	Weston et al. (2016a)
T Pyx	0.25	Nelson et al. (2014)
V723 Cas	0.24 ± 0.1	Heywood et al. (2005)
V1974 Cyg	0.46[a]	Hjellming (1996)
V351 Pup	0.74[b]	Wendeln et al. (2017)
V838 Her	0.042	Hjellming (1996)
V827 Her	0.25	Hjellming (1996)
V1819 Cyg	0.2	Hjellming (1996)
QU Vul	0.87	Hjellming (1996)
V1500 Cyg	0.036	Hjellming et al. (1979)
FH Ser	0.048	Hjellming et al. (1979)
HR Del	0.44	Hjellming et al. (1979)
median	0.25	

[a] Ivinson et al. (1993) report $v_{\rm min}/v_{\rm max} = 0.16$.

[b] Hjellming (1996) found $v_{\rm min}/v_{\rm max} = 0.069$.

Ejecta mass estimate from NuSTAR absorbing column

Model/Velocity	600 km/s	2400 km/s
Thin shell $T_0 + 36$	7.1×10^{-5} $M_\odot$	1.1×10^{-3} $M_\odot$
Thin shell $T_0 + 57$	2.4×10^{-5} $M_\odot$	3.9×10^{-4} $M_\odot$
Thin shell late ejection	8.0×10^{-6} $M_\odot$	1.3×10^{-4} $M_\odot$
Hubble flow $T_0 + 36$	1.4×10^{-5} $M_\odot$	2.3×10^{-4} $M_\odot$
Hubble flow $T_0 + 57$	4.9×10^{-6} $M_\odot$	7.8×10^{-5} $M_\odot$
Hubble flow late ejection	1.6×10^{-6} $M_\odot$	2.6×10^{-5} $M_\odot$

Ejecta mass estimate from NuSTAR absorbing column

Model/Velocity	600 km/s	2400 km/s
Thin shell $T_0 + 36$	$7.1 \times 10^{-5}\ M_\odot$	$1.1 \times 10^{-3}\ M_\odot$
Thin shell $T_0 + 57$	$2.4 \times 10^{-5}\ M_\odot$	$3.9 \times 10^{-4}\ M_\odot$
Thin shell late ejection	$8.0 \times 10^{-6}\ M_\odot$	$1.3 \times 10^{-4}\ M_\odot$
Hubble flow $T_0 + 36$	$1.4 \times 10^{-5}\ M_\odot$	$2.2 \times 10^{-4}\ M_\odot$
Hubble flow $T_0 + 57$	$4.9 \times 10^{-6}\ M_\odot$	$7.8 \times 10^{-5}\ M_\odot$
Hubble flow late ejection	$1.6 \times 10^{-6}\ M_\odot$	$2.6 \times 10^{-5}\ M_\odot$

Shell ejected on day 24

Shocks in novae

- Accelerate particles producing GeV γ-ray (and synchrotron radio) emission
- Heat plasma emitting hard X-rays

Simultaneously observing thermal and non-thermal emission from shocks we can constrain particle acceleration efficiency (Vurm & Metzger, 2018)!

Fermi/NuSTAR flux ratio on day 36

Steinberg & Metzger (2018) argue, that the shocks in novae are radiative: emit most of their energy in X-rays and spend 2% of energy or less on particle acceleration

- Measured **$L\gamma/Lx$~80, not 0.02**!
- What we see with NuSTAR is not the shock responsible for the GeV emission
- NuSTAR data are consistent with a very bright emission **$L\gamma/Lx$~0.01**... if it's soft (kT~0.5 keV):

`constant*phabs*vphabs*vapec`: $\chi^2_{\rm red} = 1.0547$, d.o.f. $= 200$, $p = 0.28$

`constant*phabs*vphabs*(vapec+vapec)`: $\chi^2_{\rm red} = 1.0292$, d.o.f. $= 196$, $p = 0.37$

Summary

- No sharp transition from hard to SSS emission
- Ejecta has **highly non-solar abundances**, includes a lot of WD material
- **CO WD** (no Mg, Ne emission)
- **Ejecta mass 10^{-5} - 10^{-6} Msun**
- Most of it **ejected 24 days after explosion**
- Hard X-rays confirm the presence of **shocks**
- Surprising **Lγ/Lx~80** ratio

Thanks!

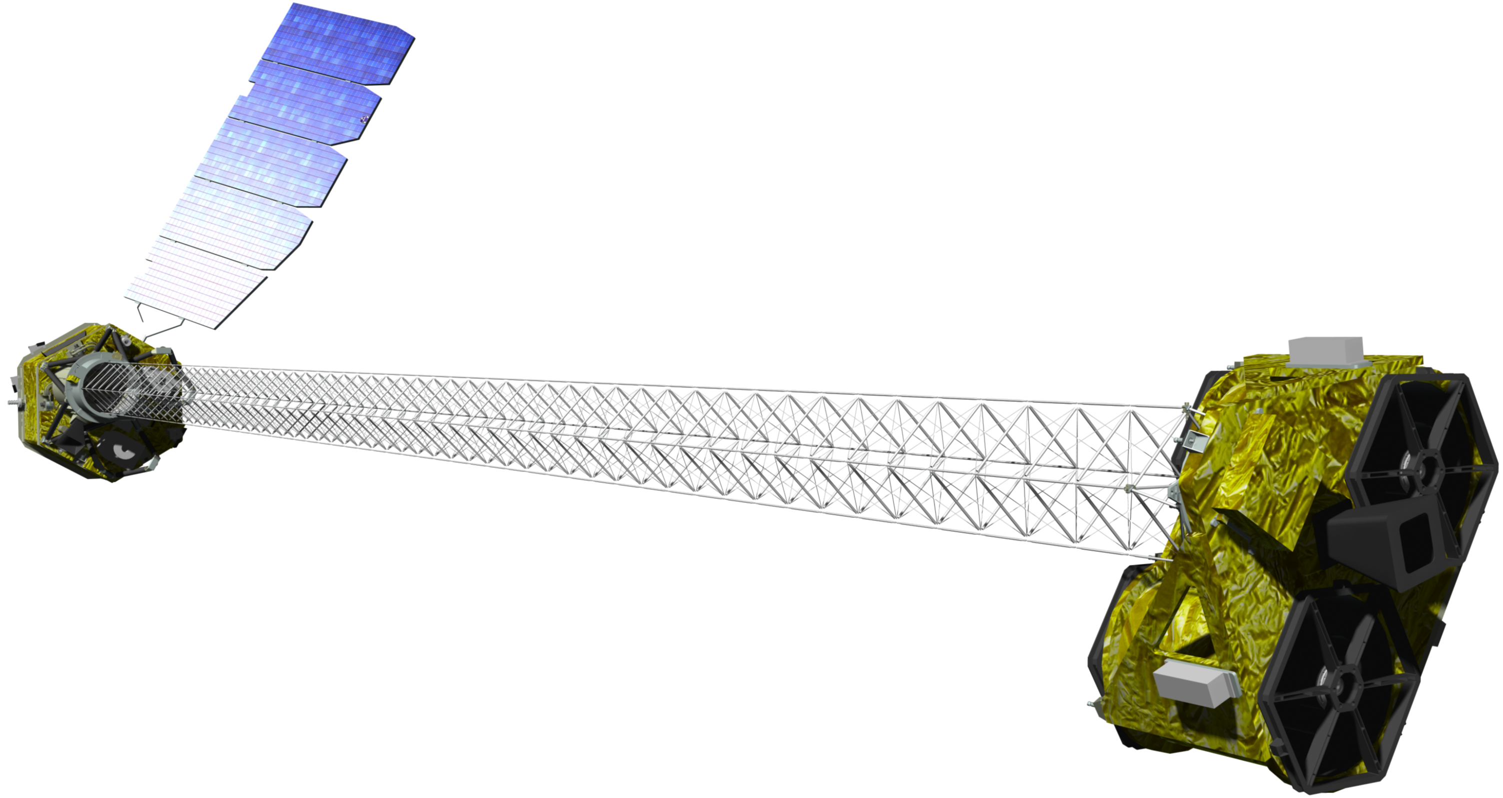

NuSTAR observations of V906 Car

NuSTAR observing log

ObsID	Epoch (days)	Start UT	Stop UT	Exposure FPMA (ks)	Exposure FPMB (ks)	Net count rate FPMA (cts/s)	Net count rate FPMB (cts/s)
80301306002	36.3	2018-04-20 14:46	2018-04-22 02:01	48.8	48.5	0.01582 ± 0.00066	0.01630 ± 0.00067
90401322002	57.2	2018-05-11 16:26	2018-05-12 18:01	47.5	47.4	0.04343 ± 0.00102	0.04184 ± 0.00101

Column designation: Col. 1 – observation identification number; Col. 2 – time since outburst; Col. 3 and 4 – start and stop time of the observation (interrupted by Earth occultations and South Atlantic Anomaly passes); Col. 5 and 6 – total on-source exposure time for FPMA and FPMB, respectively; Col. 7 and 8 – source count rate (background-subtracted) for FPMA and FPMB, respectively.

NuSTAR observations of V906 Car

Parameters of the *NuSTAR* spectral model `constant*vphabs*vapec`

Epoch (days)	N_{HI} ($\times 10^{22}$ cm^{-2})	kT (keV)	FeCoNi abundances	CNO abundances	C_{FPMB}	Model 3.5-78.0 keV flux $\log_{10}$(ergs/cm^2/s)	Unabsorbed 3.5-78.0 keV flux $\log_{10}$(ergs/cm^2/s)
Fe-deficient model: $\chi^2_{red} = 1.0281$, d.o.f. $= 199$, $p = 0.38$							
36	293.1 ± 20.3	8.04 ± 0.91	0.086 ± 0.030	1.0	1.109 ± 0.062	-11.570 ± 0.012	-11.068 ± 0.012
57	44.82 ± 2.72	4.43 ± 0.17	—”—	—”—	1.006 ± 0.034	-11.454 ± 0.007	-11.179 ± 0.007
CNO-overabundance model: $\chi^2_{red} = 1.0457$, d.o.f. $= 199$, $p = 0.31$							
36	4.287 ± 2.288	8.59 ± 0.88	1.0	209.6 ± 110.4	1.107 ± 0.062	-11.564 ± 0.012	-11.142 ± 0.012
57	0.568 ± 0.288	4.38 ± 0.17	—”—	—”—	1.006 ± 0.034	-11.454 ± 0.007	-11.221 ± 0.007
XMM-derived abundances model: $\chi^2_{red} = 1.0552$, d.o.f. $= 200$, $p = 0.28$							
36	19.30 ± 1.33	8.62 ± 0.85	0.10	$C = 0$, $O = 29$,	1.105 ± 0.062	-11.565 ± 0.012	-11.119 ± 0.012
57	2.648 ± 0.160	4.34 ± 0.17	—”—	$N = 345$	1.005 ± 0.034	-11.455 ± 0.007	-11.208 ± 0.007
XMM abundances and fixed Galactic column model: `constant*phabs*vphabs*vapec`: $\chi^2_{red} = 1.0547$, d.o.f. $= 200$, $p = 0.28$							
36	19.29 ± 1.32	8.63 ± 0.84	0.10	$C = 0$, $O = 29$,	1.1054 ± 0.062	-11.565 ± 0.012	-11.119 ± 0.012
57	2.636 ± 0.160	4.34 ± 0.17	—”—	$N = 345$	1.005 ± 0.034	-11.455 ± 0.007	-11.208 ± 0.007
Two-temperature plasma model: `constant*phabs*vphabs*(vapec+vapec)`: $\chi^2_{red} = 1.0292$, d.o.f. $= 196$, $p = 0.37$							
36	27.60 ± 4.26	6.90 ± 0.72, 0.567 ± 0.066	0.10	$C = 0$, $O = 29$,	1.116 ± 0.062	-11.540 ± 0.025	-9.599 ± 0.025
57	3.516 ± 1.483	4.05 ± 0.42, 0.579 ± 0.171	—”—	$N = 345$	1.005 ± 0.034	-11.421 ± 0.030	-11.074 ± 0.030

	Case 1 EPIC+RGS	Case 2 EPIC+RGS	Case 3 EPIC+RGS	Case 4 RGS	Case 5 RGS
PHABS					
N_H ($\times 10^{21}$ cm^{-2})	$1.8^{+0.3}_{-0.2}$	$1.8^{+0.2}_{-0.2}$	$2.4^{+0.4}_{-0.3}$	$2.1^{+0.5}_{-1.0}$	$2.0^{+2.1}_{-1.0}$
VPHABS					
N_H ($\times 10^{21}$ cm^{-2})	$0.08^{+0.02}_{-0.02}$	$0.13^{+0.03}_{-0.02}$	$0.12^{+0.03}_{-0.03}$	<0.4	<0.4
BVAPEC					
kT (keV)	$1.06^{+0.01}_{-0.01}$	$1.11^{+0.01}_{-0.01}$	$1.07^{+0.04}_{-0.01}$	$0.79^{+0.04}_{-0.10}$	$0.98^{+0.15}_{-0.12}$
redshift	$(-2.9\pm0.1)\times10^{-3}$	$(-2.9\pm0.2)\times10^{-3}$	$-2.9\times10^{-3*}$	$(-3.1\pm0.2)\times10^{-3}$	$-2.9\times10^{-3(*)}$
velocity (km s^{-1})	394±70	378±72	$378^{(*)}$	386^{+72}_{-76}	378^{*}
$N/N_\odot$	728^{+232}_{-150}	403^{+99}_{-73}	345^{+93}_{-70}	230^{+236}_{-81}	212^{+197}_{-87}
$O/O_\odot$	30^{+7}_{-6}	24^{+4}_{-5}	29^{+7}_{-5}	14^{+15}_{-5}	17^{+12}_{-5}
$Ne/Ne_\odot$	$0.7^{+0.6}_{-0.5}$	$2.3^{+0.6}_{-0.5}$	$2.2^{+0.6}_{-0.5}$	$1.1^{+1.3}_{-0.5}$	$1.5^{+1.3}_{-0.7}$
$Mg/Mg_\odot$	$1.0^{+0.2}_{-0.2}$	$0.7^{+0.2}_{-0.1}$	$0.6^{+0.2}_{-0.1}$	$1.0^{+1.0}_{-0.3}$	$0.9^{+0.6}_{-0.3}$
$Si/Si_\odot$	$1.6^{+0.4}_{-0.3}$	$1.2^{+0.2}_{-0.2}$	$1.1^{+0.2}_{-0.2}$	$1.0^{+2.1}_{-0.7}$	$2.0^{+1.3}_{-0.5}$
$Fe/Fe_\odot$	$0.17^{+0.08}_{-0.05}$	<0.1	<0.1	<0.13	<0.04
χ^2_ν	1.25	1.16	1.15	1.01	1.01
d.o.f.	1847	1488	1837	987	977

Notes:
Model CONSTANT*PHABS*VPHABS*BVAPEC in four different cases:
Case 1: in the whole spectral coverage, without Gaussian lines;
Case 2: excluding spectral regions associated with (r,i,f) lines: 0.4-0.45 keV, 0.55-0.6 keV, 0.85-0.95 keV, and 1.3-1.4 keV;
Case 3: in the whole spectral coverage, including Gaussian lines associated with r,i,f lines (Table 3);
Case 4: only RGS, without Gaussian lines;
Case 5: only RGS, with Gaussian lines associated with r,i,f lines (Table 3);
Abundance table: aspl: Asplund M, Grevesse N., Sauval A.J. & Scott P., 2009, ARAA, 47, 481;

GeV and MeV emission from novae

Review by Hernanz (2014 ASPC, 490, 319)

- E>100 MeV continuum emission detected from 14 novae by Fermi (AGILE saw one)
- MeV emission from radioactive decay predicted, but not found